Journal of Colloid and Interface Science 563 (2020) 229–240

Contents lists available at ScienceDirect

Journal of Colloid and Interface Science

journal homepage: www.elsevier.com/locate/jcis

Thermally and pH-responsive gelation of nanoemulsions stabilized by weak acid surfactants

Li-Chiun Cheng [a], Seyed Meysam Hashemnejad [a], Brady Zarket [b], Sivaramakrishnan Muthukrishnan [b], Patrick S. Doyle [a,*]

[a] Department of Chemical Engineering, Massachusetts Institute of Technology, Cambridge, MA 02139, United States
[b] L'Oréal Research and Innovation, Clark, NJ 07066, United States

GRAPHICAL ABSTRACT

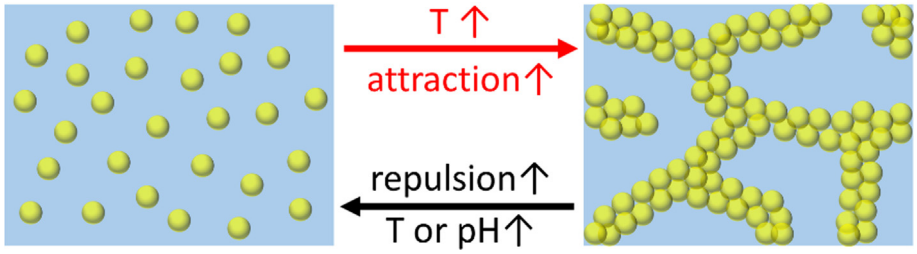

ARTICLE INFO

Article history:
Received 16 October 2019
Revised 12 December 2019
Accepted 13 December 2019
Available online 14 December 2019

Keywords:
Nanoemulsions
Colloidal gels
Weak acid surfactants
Stimuli-responsive
Rheology

ABSTRACT

Nanoemulsions are widely used in applications such as in food products, pharmaceutical ingredients and cosmetics. Moreover, nanoemulsions have been a model colloidal system due to their ease of synthesis and the flexibility in formulations that allows one to engineer the inter-droplet potentials and thus to rationally tune the material microstructures and rheological properties. In this article, we study a nanoemulsion system in which the inter-droplet interactions are modulated by temperature and pH. We develop a nanoemulsion suspension in which the droplets are stabilized by weak acid surfactants whose charged state can be independently controlled by temperature and pH, leading to a responsive electrostatic repulsion. Moreover, the additional poly(ethylene glycol) segment (PEG) on the surfactant gives rise to a temperature responsive attraction between droplets via PEG-PEG association and ion-dipole interaction. The interplay of these three interactions gives rise to non-monotonic trends in material properties and structures as a function of temperature. The underlying mechanism resulting in these trends is obtained by carefully characterizing the nanoemulsion droplets and studying the molecular interactions. Such mechanistic understanding also provides guidance to modulate the inter-droplet potential using pH and ionic strength. Moreover, the molecular understanding of the weak acid surfactant also sheds light on the destabilization of the nanoemulsion droplets triggered by a switch in pH. The control of the competition of attractive and repulsive interactions using external stimuli opens up the possibility to design complex nanoemulsion-based soft materials with controllable structures and rheological properties.

* Corresponding author.
E-mail address: pdoyle@mit.edu (P.S. Doyle).

https://doi.org/10.1016/j.jcis.2019.12.054
0021-9797/

1. Introduction

Nanoemulsions are kinetically stable liquid-liquid suspensions where one immiscible liquid disperses in another with droplet size on the order of 10–100 nm. The nanoscale droplet size leads to robust stability, large interfacial area and optical transparency, which has made nanoemulsions a popular topic in the field of colloidal and interface science for the past two decades [1]. Moreover, the small lipophilic domains can be further utilized in applications such as nano-reactors for polymerizations [2,3] or nano-cargos in food products [4–6]. The other important feature of nanoemulsions is the ease of synthesis in which new formulations can be easily synthesized. Such flexibility allows researchers to modulate the interactions between droplets and hence the material properties, making nanoemulsion a versatile material in diverse fields such as in sensors [7,8], cosmetics [9], and the complex material design [10]; and a compelling model system for studying colloidal behavior such as suspension rheology [11], self-assembly [12] and gelation [13].

Nanoemulsions that undergo gelation have attracted much attention in both fundamental studies [13–15] and practical applications [16,17]. Gelation of nanoemulsions, or for general colloidal suspensions, is controlled by modulating the interactions between the droplets, and the gelation can be induced by manipulating either attractive or repulsive interactions. For attraction-driven gelling systems, one common way to induce gelation is via a depletion interaction. By adding depletants to the continuous phase, these non-adsorbing species are excluded from the vicinity of the droplets, leading to an imbalance in the osmotic pressure. This osmotic pressure acts as a net attractive force between the droplets, ultimately giving rise to the gelation [18,19]. Different depletants including surfactant micelles [20,21] and non-adsorbing polymers [17] have been used to obtain gelling nanoemulsions. On the other hand, gelation of nanoemulsions can also be induced by modulating repulsions. Perhaps the most widely seen approach is the screening of electrostatic repulsion by adding the electrolytes into charged-stabilized nanoemulsion suspensions. The addition of electrolytes reduces the effective length scale of the electrostatic repulsion, leading to the emergence of a secondary minimum in the interactive potential and eventually inducing the gelation [22,23]. Another example utilizing electrostatic repulsion, so-called repulsive gelation [21], to obtain nanoemulsion gels is through the increase of effective oil volume fraction in electrostatically-stabilized emulsion systems [12,24]. The effective oil volume fraction (ϕ_e) is calculated by considering the actual oil volume fraction (ϕ_a) and the excluded volume resulted from the repulsive charge cloud that extends from the oil/water interface (i.e. Debye length, κ^{-1}), and $\phi_e = \phi_a(1 + \kappa^{-1}/a)^3$ where a is the droplet radius. As the droplet size decreases, ϕ_e increases. When ϕ_e is greater than the maximum random jamming limit, a viscoelastic nanoemulsion gel is obtained.

Our group has been designing and studying nanoemulsion systems in which gelation is triggered by an external stimulus — an increase in temperature [25–27]. By understanding the inter-droplet interactions at a molecular level, we have designed various thermally-gelling nanoemulsions in which the system experiences a sol-gel transition at elevated temperatures. For example, by adding telechelic oligomers where both ends of the hydrophilic backbone are functionalized with hydrophobic moieties to the continuous phase, the oligomers act to bridge droplets upon increasing the temperature and ultimately lead to gelation [25,28]. On the other hand, we also designed another thermally-gelling mechanism by including non-ionic amphiphilic oligomers in charged-stabilized oil-in-water nanoemulsions [26]. At elevated temperatures, the non-ionic oligomers replace the ionic surfactants on the droplets. Such displacement leads to a dramatic decrease in the electrostatic repulsion and gives rise to gelation. Finally, we also developed a gelling nanoemulsion by adding a small-amount of Pluronic copolymers to the continuous phase. We hypothesized that the gelation at elevated temperatures is induced through jamming via the formation of copolymer micelles and the increase of ϕ_e by the adsorption of copolymers onto the droplets [27]. Overall, these external-stimuli responsive systems enhance the ability for material processing and manipulation, which benefits not only the fundamental research such as studying the effect of processing history on the material behaviors [29] but also practical applications such as the design of hierarchical structured hydrogels [16]. However, for both fundamental studies and applications, it would be desirable to develop systems that respond to another stimulus in addition to temperature. For example, systems that are responsive to the change of pH can be utilized for skincare products [30,31] or enhanced oil recovery [32].

Here, we report a gelling nanoemulsion system in which the material properties are responsive to temperature and pH. The nanoemulsion is synthesized through a low-energy route, and the droplets are stabilized using a weak acid surfactant containing a PEG segment and a carboxyl group. The deprotonation of the carboxyl group greatly influences the behavior of the nanoemulsion. The material behavior is characterized by rheometry and confocal microscopy [33–38]. This new nanoemulsion system shows a non-intuitive behavior that is very different from all of the prior thermally-gelling systems our group has studied. At elevated temperatures, the viscoelastic moduli first increase, then decrease and finally increase again, and the microstructures of the assembled nanoemulsion also show the same non-monotonic trend. This non-intuitive trend is explained by the non-monotonic increase in the net attraction due to the competition between repulsive and attractive interactions, which are investigated by measuring the zeta potential of the nanoemulsion droplets and comparing our system with the studies in the literature. We hypothesize that the association between PEG segments and charged carboxylate groups are responsible for the changes in the inter-droplet interactions. Armed with this mechanistic understanding, we further show that the thermally-responsive rheological properties of the nanoemulsion can be modulated through the change of pH and ionic strength. Moreover, with the knowledge of the molecular geometry of the surfactants, we also demonstrate that the nanoemulsion droplets can be destabilized by changing the pH of the system. This work opens up the opportunity to design multi-stimuli responsive nanoemulsion systems by controlling the chemical moieties of the surfactants adsorbed on the droplets.

2. Materials and methods

2.1. Materials

Isopropyl myristate (IM, purity $\geq$ 98%), laureth-11 carboxylic acid ($M_n \approx$ 690 g/mol, impurities: NaCl $\leq$ 1.5%, water = 8–12%), lauric acid (purity $\geq$ 98%), sodium hydroxide (NaOH, purity $\geq$ 97%), sodium chloride (NaCl, purity $\geq$ 99%) and Nile Red (purity $\geq$ 98%) were purchased from Sigma Aldrich. Poly(ethylene glycol) (PEG400, M_n = 400 g/mol, purity $\geq$ 98%) was purchased from TCI Chemicals. All chemicals were used without further purification.

2.2. Nanoemulsion synthesis

The oil-in-water nanoemulsion contained IM droplets (weight fraction ϕ = 12.5 wt%) stabilized by a mixture of carboxylic

acid-based surfactants composed of laureth-11 carboxylic acid (12.5 wt%) and lauric acid (3.13 wt%), and a co-surfactant PEG400 (9.38 wt%) [27] suspended in the de-ionized water. The hydrophilic-lipophilic balance (HLB) of the mixed surfactant is 13. We have also demonstrated that it is important to use the co-surfactant to stabilize the nanoemulsion by measuring the size of the droplets over time at various PEG400 concentrations (Fig. S1).

We used the Phase Inversion Composition (PIC) method to synthesize the nanoemulsions which provides a low-energy route to obtain nano-sized droplets [1]. For synthesis, a homogeneous oil mixture containing IM, surfactants and co-surfactants was first prepared. Next, the de-ionized water was added drop-wisely into the oil mixture under a constant stirring using a magnetic stirrer bar. The stirring speed was kept at 1100 rpm throughout the synthesis. This approach is called the PIC method since the continuous phase is added into the disperse phase. During the addition, at some critical point which is known as phase inversion point, the oil-water interface experiences an ultra-low interfacial tension which facilitates the formation of nano-sized droplets [39,40]. We measured the droplet size and the polydispersity by using dynamic light scattering (90Plus PALS, Brookhaven Instruments) after diluting the nanoemulsion to ϕ = 0.5 wt% using de-ionized water. In our system, the resulting droplet diameter is 20 nm with a polydispersity $\approx$ 0.08.

2.3. pH measurement

The pH of nanoemulsions was measured using a pH meter (Orion Star™ A215, ThermoFisher Scientific) equipped with an Orion™ ROSS Ultra™ Refillable pH/ATC Triode™ electrode. All the measurements were performed at 20 °C. For the different pH values studied in this work, pH was adjusted using NaOH. The reported pH values were obtained by measuring the pH of the whole nanoemulsion suspension (both continuous phase and the droplets).

2.4. Rheological characterization

The rheological properties of the nanoemulsion were measured by using a stress-controlled rheometer (DHR-3, TA instrument) equipped with a 2° 40 mm upper-cone and a temperature-controlled Peltier lower-plate. To prevent evaporation of the sample, a solvent trap was used and a few drops of water were added on top of the cone. Before each measurement, a conditioning procedure was applied to the sample: a pre-shear step was applied by performing a constant rotation at a speed of 10 rad/s for 30 s, followed by a 60-second period where the sample stayed quiescently on the rheometer. The whole conditioning step was kept at 20.0 °C in order to eliminate any possible thermal history effect [29]. In the pre-shear step, no gelation or self-assembly of the nanoemulsion suspension is obtained (as shown in Figs. 1 and 2 where the rheology is reported, and Fig. 3 where the confocal images are reported). Therefore, this pre-shear step has no influence on the gel structures and the associated rheological properties when the temperature is increased.

Frequency-sweep and temperature-ramp measurements were performed using small-amplitude oscillatory shear (SAOS) at a shear strain γ = 0.05%. For frequency-sweep measurements, the storage modulus, G′, and the loss modulus, G″, at various temperatures, T, with angular frequency ω = 1–100 rad/s were measured. Before each measurement, the temperature was kept at the target T for 30 min. For temperature-ramp measurements, G′ and G″ were measured as a function of temperature at a fixed angular frequency ω = 25 rad/s. The nanoemulsion droplets stay stable over the experimental temperature window by monitoring the droplet size as a function of temperature (Fig. S2). For each measurement, the fresh nanoemulsion was loaded on the rheometer.

2.5. Zeta potential

Zeta potentials of the nanoemulsion droplets with different temperatures and pH were measured by a Brookhaven Instruments 90Plus PALS zetasizer. Before each measurement, the mother

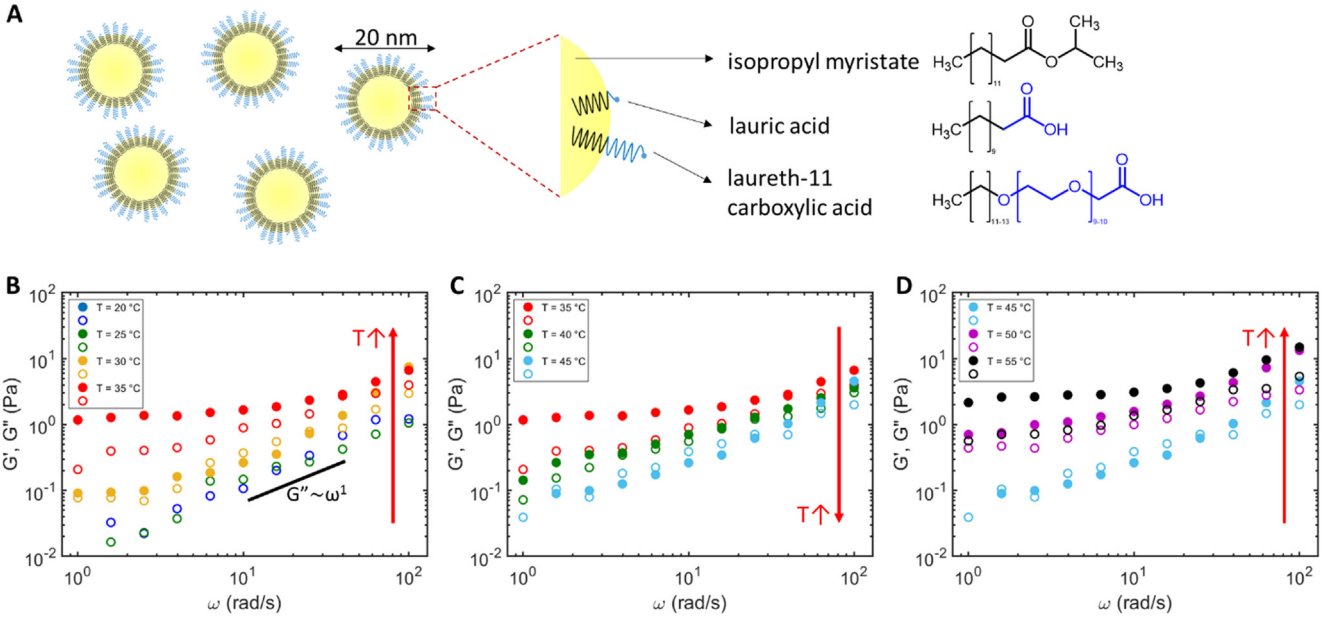

Fig. 1. Schematic of the nanoemulsion suspension and the linear viscoelastic moduli (closed: G′, open: G″) as a function of angular frequency (ω) at elevated temperatures. The pH of the nanoemulsion is 2.5. (A) The schematic of the nanoemulsion suspension. Upon increasing the temperature, viscoelastic moduli (B) first increase, (C) then decrease, and (D) finally increase again.

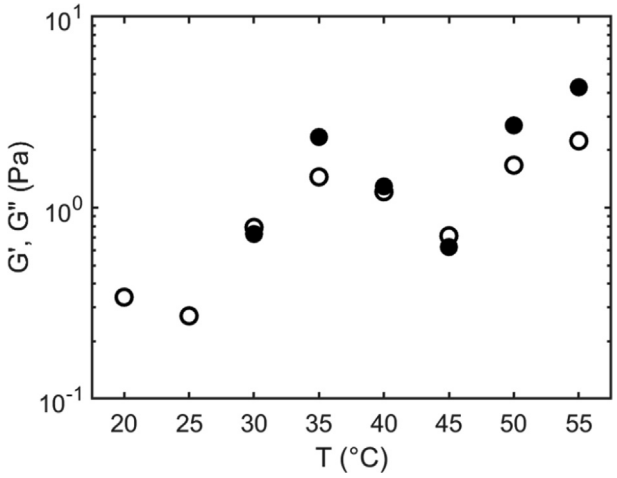

Fig. 2. Linear viscoelastic moduli (closed: G′, open: G″) as a function of temperature at an angular frequency ω = 25 rad/s from Fig. 1 (see Fig. S3 with data with error bars).

nanoemulsion (ϕ = 12.5 wt%) was freshly diluted to ϕ = 0.5 wt%. For each measurement, the fresh nanoemulsion was loaded.

2.6. Confocal microscopy

The microstructures of the assembled nanoemulsion at various temperatures were captured using a confocal laser scanning microscope (LSM 700, Zeiss) equipped with a 63× oil-immersion objective. The temperature was controlled using an objective warmer (OW-1, Warner Instruments) and a microscope heating stage (Heating Insert P S1, Zeiss) equipped with a temperature controller (TempModule S1, Zeiss). The temperature was independently calibrated by an additional digital thermometer (#51 II, Fluke).

For visualization, IM was fluorescently labeled by dissolving Nile Red in IM at a concentration of 0.1 mg/g before the nanoemulsion synthesis. The spatial resolution of the confocal microscope is ≈ 200 nm. Therefore, the individual nanoemulsion droplets (size range from 20 to 110 nm) cannot be detected. To visualize the microstructures, the nanoemulsion was loaded in a homemade cylinder-shaped glass chamber using Secure-Seal™ spacers. The resulting chamber is with a height ≈ 500 μm and a diameter ≈ 9 mm. A small diameter ensures the thermal homogeneity throughout the sample [41]. Before the images were taken, the nanoemulsion-filled chamber was mounted on the heating plate at the target T for 30 min. Fresh samples were used for each rheological characterization and confocal imaging (i.e. the samples after rheological measurements were discarded and not reused for confocal imaging).

3. Results and discussion

3.1. Thermally-responsive nanoemulsions

Our nanoemulsion is a liquid at room temperature, but transitions into a viscoelastic gel upon heating. However, when the temperature (T) is further increased, the mechanical strength decreases and then increases again. We quantitatively studied this interesting phase behavior using the small-amplitude oscillatory shear rheometry. Fig. 1 shows the schematic of the nanoemulsion suspension and the dynamic viscoelastic moduli (storage modulus G′ and loss modulus G″) as a function of angular frequency (ω) at elevated temperatures. At T = 20 and 25 °C, the nanoemulsion shows a liquid behavior where G″ (ω) ~ ω^1 [42]. When T is

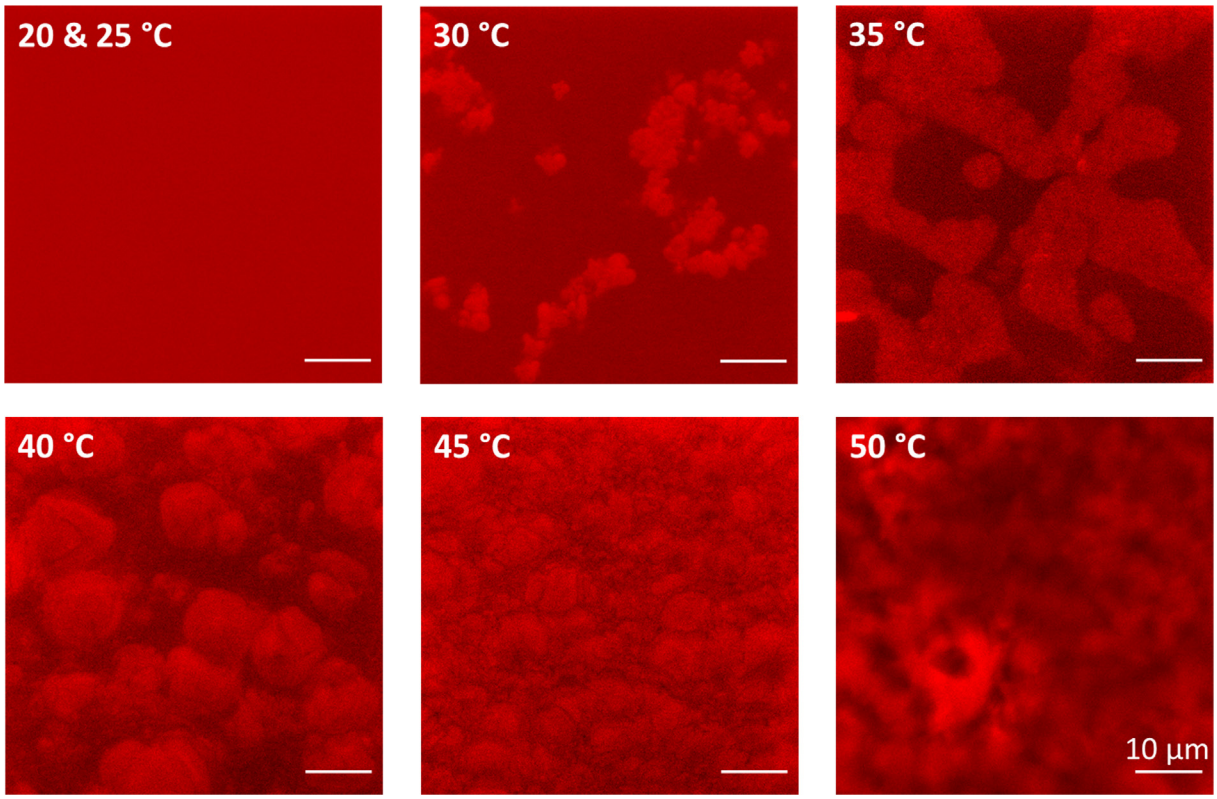

Fig. 3. Microstructures of the nanoemulsion (pH = 2.5) at elevated temperatures using confocal microscopy. The oil droplets are fluorescently labeled using Nile Red. Scale bars = 10 μm. (For interpretation of the references to colour in this figure legend, the reader is referred to the web version of this article.)

increased, G′ (ω) and G″ (ω) increase and the system undergoes a sol-gel transition. Eventually, G′ (ω) is larger than G″ (ω), suggesting the nanoemulsion has transitioned from a liquid at room temperature to a viscoelastic gel at T = 35 °C.

Surprisingly, G′ and G″ decrease as T is further increased, as shown in Fig. 1C. The trend in the viscoelastic moduli as a function of temperature can be more clearly seen in Fig. 2. The decrease in G′ and G″ remains until T reaches 45 °C. However, when T is further increased, G′ and G″ increase again, and such increase remains within our experimental temperature window, as shown in Fig. 1D and Fig. 2. We also noticed that the gel strength of this nanoemulsion (the largest G′ is ~ 10^0 to 10^1 Pa) is significantly smaller than the prior thermally-gelling nanoemulsions our group has developed (G′~ 10^4 to 10^5 Pa) [25–27]. The data reported in Fig. 2, as well as Fig. 1, are all above the rheometer's torque limit. Data that cannot be measured are not presented (e.g. the storage modulus G′ at T = 20 and 25 °C). We also show that the trend in Fig. 2 is statistically significant as the change in viscoelastic moduli is well above the standard errors (Fig. S3).

3.2. Direct visualization of microstructures

Rheological properties of materials are dictated by their microstructures. Here, the microstructure of the nanoemulsion as a function of temperature was captured by confocal microscopy. Representative confocal images of self-assembled nanoemulsions are shown in Fig. 3. The oil droplets are fluorescently labeled using Nile Red. At room temperature, the image shows a red blur, suggesting that nanoemulsion droplets are homogeneously dispersed in the continuous phase. This is because the resolution limit of our confocal microscopy setup is ≈ 200 nm at which single droplets (diameter = 20 nm) cannot be visualized. When T is increased to 30 °C, a connected network begins to form, corresponding to the rheological sol-gel transition observed in Fig. 1B. While it is difficult to obtain 3D reconstructed images of the assembled microstructures by confocal microscopy due to turbidity, the 2D images suggest that the network is very sparse. This observation is similar to our prior work on a different thermally-gelling nanoemulsion which also shows a very sparse gel network in 2D confocal images near the gel point [41]. At T = 35 °C, a well-connected gel network is observed, which is again consistent with the viscoelastic gel from Fig. 1B.

When T is continuously increased to 40 and 45 °C, the gel network appears to break down into separate domains. The broken network is exhibited as cloud-like structures in Fig. 3 at T = 40 and 45 °C. This visual breakup of the network is consistent with the rheological response shown in Fig. 2 where the viscoelastic moduli decrease when T is increased from 35 to 45 °C. Finally, when T is further increased to 50 °C, remarkably, the nanoemulsion again assembles into a well-connected gel network, corresponding to the recovery of the viscoelastic moduli in Fig. 2 when T is increased to 50 °C and above.

3.3. Proposed mechanism of nanoemulsion gelation

Colloidal gelation is a result of the competition between attractive and repulsive interactions. Colloidal suspensions, as well as nanoemulsions, gel when the attractive interaction overcomes the repulsive interaction. Therefore, the non-intuitive trend in the viscoelastic moduli of our nanoemulsion (Figs. 1 and 2) suggests a non-monotonic increase in the net attraction due to the competition between attractive and repulsive interactions between nanoemulsion droplets as a function of temperature. In the following text, we will discuss the sources of both interactions.

3.3.1. Repulsive interaction

In our system, the nanoemulsion droplets are stabilized by carboxylic acid surfactants (12.5 wt% laureth-11 carboxylic acid and 3.13 wt% lauric acid). At room temperature, the weak acid surfactants are uncharged and the PEG segments on droplets provide the steric repulsion that gives rise to the colloidal stability of the nanoemulsion. However, this steric repulsion is most likely not responsible for the increase in the repulsive interaction as a function of temperature as the number density of the surfactant is not modulated. Therefore, we hypothesized that the dissociation of the carboxylic acids leads to a temperature-dependent electrostatic repulsion between the droplets, as illustrated in Fig. 4A. To validate this hypothesis, we measured the zeta potential (ζ) of the nanoemulsion droplets as a function of temperature, and the result is shown in Fig. 5A. At room temperature, the droplets are nearly uncharged, suggesting the dissociation of the carboxyl group is negligible. However, as the temperature is increased to 35 °C, a decrease in ζ is observed. Such decrease indicates the dissociation of the carboxyl group is promoted when the temperature is increased, and the negative value of ζ strongly supports that it is the residual carboxylate group on the droplet that gives rise to the surface charge, and hence the increase in the magnitude of ζ, of the nanoemulsion droplets. Consistent with our results, it has been reported in the literature that the dissociation of carboxylic acids [43–46], as well as other weak acids [47], is enhanced at elevated temperatures.

The trend of decreasing ζ as a function of temperature is consistent with the trend of viscoelastic moduli. In Fig. 5A, ζ remains nearly zero from T = 20 to 30 °C, starts to decrease from T = 30 to 35 °C, experiences a large decrease from T = 35 to 45 °C and finally reaches a plateau when T ≥ 45 °C. This trend in ζ is consistent with the viscoelastic moduli in Fig. 2. Starting from room temperature, first, G′ and G″ experience an initial increase. During this initial period, the electrostatic repulsion should be negligible since ζ is nearly zero, and the increase in viscoelastic moduli and the formation of assembled gel network (Fig. 3) are presumably due to the increase in attractive interaction between droplets. The details of the attraction will be discussed later. Next, ζ undergoes a dramatic decrease, hence the increase in the electrostatic repulsion, when T is increased to 45 °C, and the viscoelastic moduli decrease within the same temperature range in Fig. 2. This decrease in G′ and G″ suggests the repulsion overcomes the attraction. Finally, as the temperature is further increased, ζ reaches a plateau, leading to a nearly constant electrostatic repulsion. In this regime, G′ and G″ meet their second increase and the gel network is again exhibited (Fig. 3), indicating the attractive interaction overcomes the electrostatic repulsion in the high-temperature regime, as in the initial period (T = 20 to 30 °C).

Thus far, we have demonstrated that our nanoemulsion system has an electrostatic repulsion which is modulated by temperature. By comparing trends in the zeta potential to the trends observed in the rheological measurement, we propose that there must be competing attractive interactions. In the next section, we will discuss the origin of the attractive interactions in our system.

3.3.2. Attractive interaction

By considering the constituents of our nanoemulsion, we believe there are two sources that are responsible for the attractive interaction between the droplets: (1) the ion-dipole interaction between the charged carboxylate group and the poly(ethylene glycol) segment (PEG) on laureth-11 carboxylic acid, and (2) the association between PEGs on the laureth-11 carboxylic acids between droplets. A schematic diagram of both mechanisms is shown in Fig. 4B. For clarification, free PEG in the continuous phase (M_w = 400 g/mol) is denoted as PEG400, and the PEG on the weak-acid surfactant (M_w ≈ 400–440 g/mol) is denoted as PEG_w.

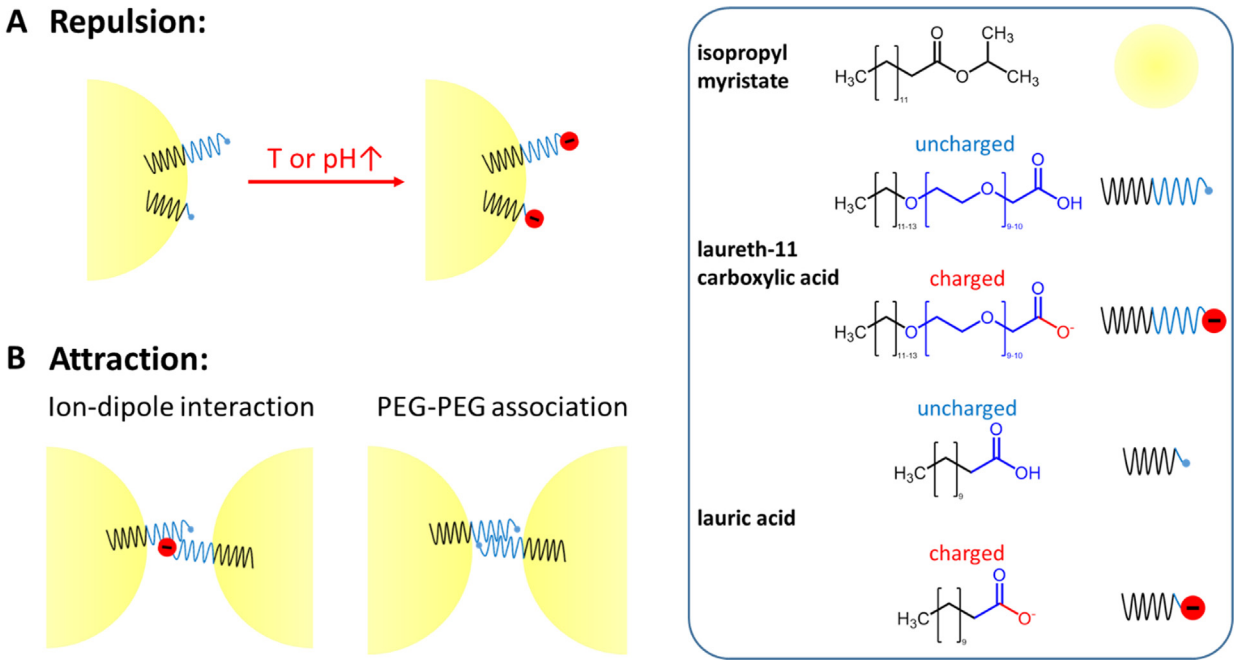

Fig. 4. Schematic of the sources of repulsive and attractive interactions in the system. (A) Repulsive interaction is from the deprotonation of the carboxylic group on the surfactant molecules absorbed on the nanoemulsion droplets. (B) Attractive interactions are from (1) the ion-dipole interaction (ion-induced dipole interaction) from the carboxylate groups and PEG segments on the surfactants, and (2) PEG-PEG association from the PEG segments on laureth-11 carboxylic acids.

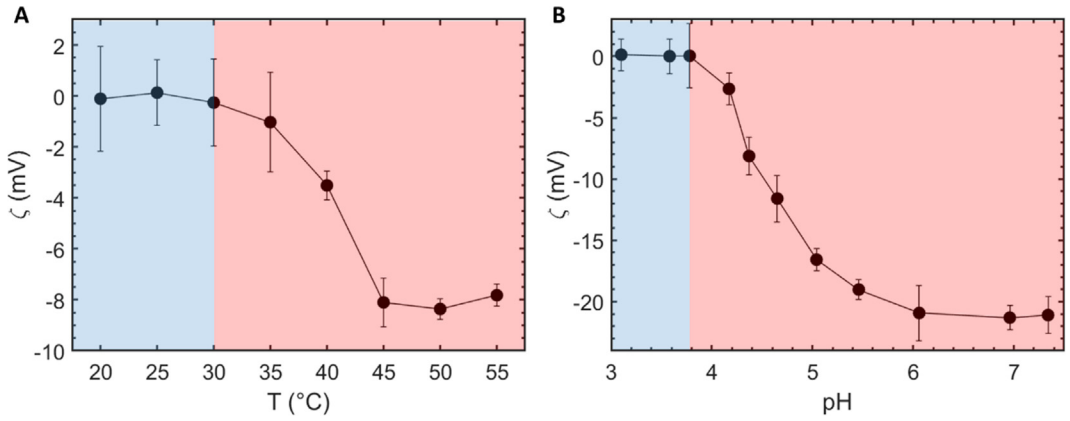

Fig. 5. Zeta potential (ζ) of the nanoemulsion droplets as a function of (A) temperature, T and (B) pH at T = 20 °C. pH was adjusted using NaOH. The pH of the nanoemulsion in (A) is 3.1. The error bars are standard errors from 30 measurements.

The ion-dipole interaction (ion-induced dipole interaction) results from the interaction between the ionic carboxylate group and PEG_w on the uncharged laureth-11 carboxylic acids. As shown in Fig. 5A, the increased temperature leads to the dissociation of the carboxyl group of the surfactant adsorbed on the droplet. However, as we will discuss the effect of pH on the system later, only a fraction of the carboxyl groups on the nanoemulsion droplets is deprotonated even at high temperatures. Therefore, the PEG_w on the undissociated laureth-11 carboxylic acids on one droplet can interact with the ionic carboxylate groups on the other droplet (Fig. 4B), giving rise to a net attraction between droplets. Indeed, the ion-dipole interaction between the charged headgroups of the surfactants and the uncharged hydrophilic moieties of polymers has been extensively studied in the literature [48]. Experimental techniques including rheometry [49], neutron scattering [50], isothermal titration calorimetry [51,52], NMR [52] and potentiometric titration [53], as well as thermodynamic models [54] and simulations [55], have strongly supported the concept of ion-dipole association.

To the best of our knowledge, the ion-dipole interaction between charged carboxylate groups and PEGs has not been systematically studied in the literature. However, it has been shown that the ion-dipole interaction not only takes place in the well-known SDS/PEG system [50–53,55], but also in other systems where uncharged polymers, such as PEG or poly(*N*-vinylpyrrolidone), are mixed with charged species such as free ions and cetyltrimethylammonium bromide (CTAB) [48,49,56,57]. These prior works demonstrate that the ion-dipole interaction is generic and should also take place in our case where the charged carboxylate groups coexist with uncharged PEGs.

The other proposed attractive interaction between nanoemulsion droplets is from the PEG_w-PEG_w association. It has been widely observed in the literature that PEG becomes more hydrophobic in aqueous solutions when the temperature is

increased [58–61]. For such aqueous PEG solutions, when the temperature is elevated, the affinity between PEGs is increased and the phase separation can be induced (i.e. a lower critical solution temperature, LCST, can be defined) [62,63]. This affinity could give rise to a net attractive interaction between the nanoemulsion droplets via the PEG_w on laureth-11 carboxylic acid (Fig. 4B). Such attraction using the LCST behavior of polymers has been utilized to induce the gelation of block copolymer colloids [64]. On the other hand, the UCST behavior has also been utilized to induce colloidal gelation in polymer-grafted nanoparticle suspensions [65,66].

For linear PEGs (such as in our system), it has been found that the temperature to induce a cloud point is higher for shorter PEG molecules [59,61,62], as the affinity between PEGs is strengthened when the molecular weight is increased. Therefore, considering the short PEG_w backbone, our system will never achieve the LCST under our experimental conditions. However, it does not mean that PEG-PEG association does not take place when the temperature is below the LCST. It has been proposed that the enhanced PEG-PEG affinity at rising temperature in water is due to the conformational equilibrium in the segments [63]. The segments prefer the polar conformations (i.e. water is a good solvent) at lower temperatures and prefer the nonpolar conformations at higher temperatures (i.e. water is becoming a poor solvent). Importantly, it has been shown that such conformational change in the segments is gradual at elevated temperatures. Bjoerling et al. have studied the conformational adaption of the PEG chains using ^{13}C NMR [59]. They found out that even for the short PEG (M_w = 600 g/mol), the segment undergoes a gradual conformational change at T = 25 to 75 °C, which is consistent to our experimental temperature window (T = 25 to 55 °C) and supports our proposed mechanism that PEG-PEG association can give rise to an attractive interaction in our system.

Bridging interaction mediated by free PEG400 in the continuous could also take place. We speculate that PEG400 does not play a major role in inter-droplet interactions. In our proposed mechanism, the attraction is from the ion-dipole interaction and PEG_w-PEG_w association between surfactants on different droplets. However, based on this proposed mechanism, we do not want to rule out the possibility that PEG400 can bridge the nanoemulsion droplets via these attractive interactions by chaining the molecules such as PEG_w-PEG400-PEG_w or COO^--PEG400- COO^-.

Overall, in our system, we believe the competition of the temperature-dependent attraction and repulsion between the nanoemulsion droplets is responsible for the non-monotonic trend in the viscoelasticity moduli (the moduli first increase, then decrease and finally increase again as temperature increases). When the repulsion dominates in the system, the gelation is diminished and hence the decrease in the viscoelastic moduli. On the other hand, when the attraction dominates, the viscoelastic moduli increase. By carefully considering the constituents of the system, we propose the attraction comes from the PEG_w-PEG_w association and the ion-dipole interaction (COO^--PEG_w). Therefore, comparing with the rheological data in Fig. 2, we have concluded that the decrease in the moduli at T = 35 to 45 °C is due to the significant increase in the zeta potential (and hence the electrostatic repulsion). Based on the zeta potential data, it can be then concluded that the second increase in the viscoelastic moduli ($T \geq 45$ °C) is primarily due to the increased PEG_w-PEG_w association. Since the zeta potential (and hence the charge density of the droplets) stays unchanged within this temperature window, we do not expect an increase in the ion-dipole interaction at $T \geq 45$ °C as no significant evidence in the literature suggests this interaction is affected by temperature. Finally, in the first gelation regime (T = 20 to 35 °C), the gelation is due to both ion-dipole interaction (since the magnitude of the zeta potential increases) and PEG_w-PEG_w association.

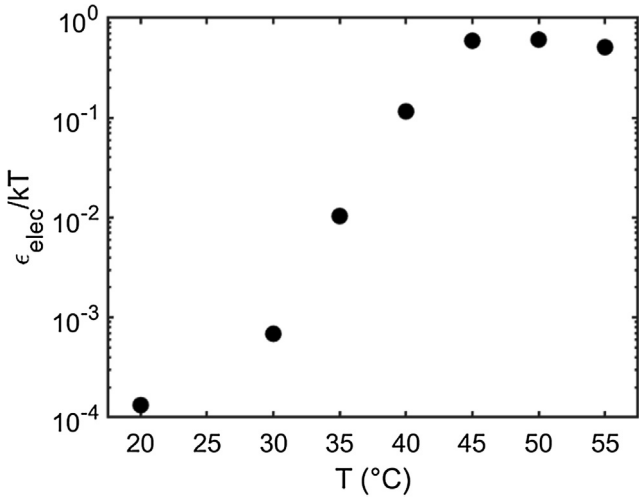

Fig. 6. The strength of the electrostatic repulsion, ε_{elec}, as a function of temperature using zeta potential reported in Fig. 5A.

As depicted in Fig. 4, the ion-dipole and PEG_w-PEG_w interactions rely on different regions of the surfactant molecules. Therefore, the interactions are highly coupled and it is very difficult to isolate the dominance between PEG_w-PEG_w association and the ion-dipole interaction (COO^-- PEG_w). Although the two interactions are difficult to decouple and immediately unclear due to the lack of a well-developed model, we can gain some understanding of their combined strength by estimating the electrostatic repulsion which they must overcome to gel the suspension. Using the zeta potential data in Fig. 5, we can estimate the strength of the electrostatic repulsion, ε_{elec}, as [26]

$$\varepsilon_{elec} = 32\pi\varepsilon_o\varepsilon_r\left(\frac{kT}{ze}\right)^2 \operatorname{atanh}^2\left(\frac{1}{4}\frac{ze\xi}{kT}\right) \quad (1)$$

where ε_o is the electric permeability of free space, ε_r is the dielectric constant of the continuous phase (here ε_r of water is used for estimation), k is Boltzmann constant, T is the absolute temperature, e is the elementary charge, z is the charge number and ξ is the zeta potential. The results are shown in Fig. 6, and reveal that the electrostatic repulsion in our system is quite weak. Even for the strongest electrostatic repulsion, ε_{elec} is only $\approx 0.6\ kT$ ($T \geq 45$ °C). Moreover, as shown in Figs. 1 and 2, the mechanical strength of this nanoemulsion gel is very weak (G' is $\sim 10^0$ to 10^1 Pa), as compared to other nanoemulsion gels our group has developed ($G' \sim 10^4$ to 10^5 Pa) where stronger attractive interactions were introduced to the nanoemulsion suspensions [25–27], suggesting the competing attractive interactions (PEG_w-PEG_w association and ion-dipole interaction) are also very weak.

3.4. Effect of pH on the rheological properties

We have shown that temperature can be used to control protonation of the carboxyl group of the surfactant on the droplet (Fig. 5A), and the resulting change in the electrostatic repulsion significantly affects the rheological response of the nanoemulsion gel (Figs. 1 and 2). However, to control the protonation of weak acids, a more straightforward way is to adjust the pH of the system. In this section, we investigate the effect of pH on the nanoemulsion suspension by studying the zeta potential of the droplets, rheological response and the droplet stability as a function of pH.

The zeta potential (ζ) of the nanoemulsion droplets as a function pH is shown in Fig. 5B. As expected, ζ decreases ($|\zeta|$ increases) with increasing pH since the deprotonation of the

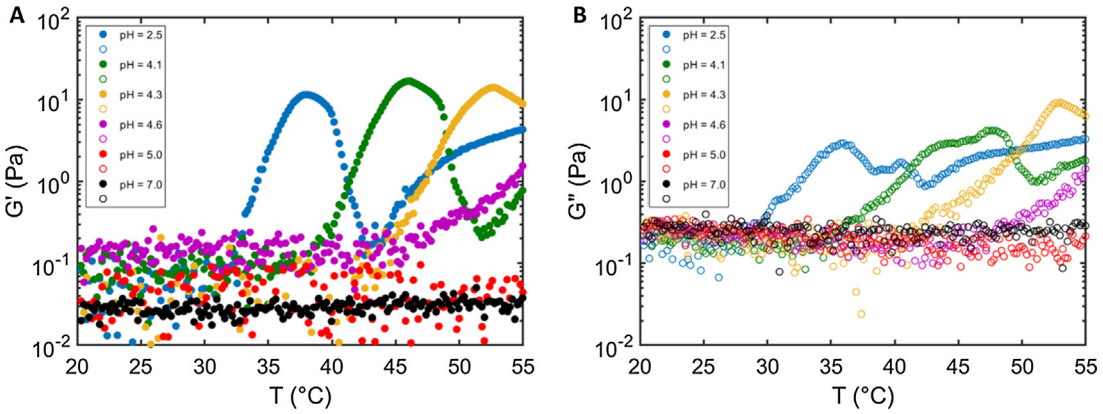

Fig. 7. Effect of pH on the rheological properties of the nanoemulsion using SAOS at a fixed angular frequency = 25 rad/s. The figure shows (A) storage modulus, G′ and (B) loss modulus, G″ as a function of temperature, T, at various pH values. pH was adjusted using NaOH.

carboxyl group is facilitated at the basic condition. Starting from the pristine nanoemulsion (pH = 3.1), ζ stays nearly zero until the pH is elevated to 3.8, and then experiences a significant decrease when pH > 4. This change in ζ is consistent with the reported pKa of laureth-11 carboxylic acid in the literature where the apparent pKa is determined to be ≈ 4 using potentiometric titration [67], and laureth-11 carboxylic acid is the major surfactant in our system. As the pH is further increased (pH > 6), ζ reaches a plateau, suggesting the deprotonation of the carboxylic acid is complete. The magnitude of the final ζ from Fig. 5B ($\zeta \approx -23$ mV, the effect of pH) also suggests that only partial deprotonation of the carboxylic acid is achieved by thermal energy ($\zeta \approx -8$ mV) as shown in Fig. 5A.

We then investigated the effect of pH on the nanoemulsion rheology. The viscoelastic moduli during a temperature ramp are shown in Fig. 7. It should be noted that for the pristine nanoemulsion in Fig. 7, pH is 2.5, which is lower than the pH of the 'pristine' nanoemulsion for the zeta potential measurement in Fig. 5B where the pH is 3.1. This difference is due to the required dilution for the zeta potential measurement, in which the nanoemulsion is diluted from 12.5 wt% (Fig. 7) to 0.5 wt% (Fig. 5B). In Fig. 7, when pH is increased, the increase in the G′ and G″ takes place at higher temperatures, indicating a higher gelation temperature is required when the pH is higher. Moreover, when pH is ≥ 5, no gelation can be induced within the experimental temperature window. The increase in pH weakens the thermally-gelling behavior of the nanoemulsion system, and this is expected since the electrostatic repulsion from the dissociation of the carboxylic acids plays an important role in the rheological response, as discussed previously. Compared with temperature, pH is a more effective strategy to promote the deprotonation of the carboxylic acid as more negative ζ can be obtained (Fig. 5B). Therefore, it is not surprising that pH significantly suppresses the gelling behavior.

We have to emphasize that the temperature-ramp rheology shown in Fig. 7 is different from the data shown in Fig. 2 where the G′ and G″ are reported at a fixed angular frequency using frequency-sweep measurements at various temperatures (temperature-jump). Our group has previously studied the effect of the thermal history on the rheological properties of thermogelling nanoemulsions in great detail, in which the temperature-ramp route can effectively build up the strength of the gel [29]. Therefore, we did expect that there will be a difference in viscoelastic moduli between Figs. 2 and 7 of the pristine nanoemulsion (pH = 2.5). Here the rheological characterization using a temperature ramp is used as a strategy to conveniently obtain a quantitative understanding of the effect of pH on the nanoemulsion rheology over a wide range of temperatures.

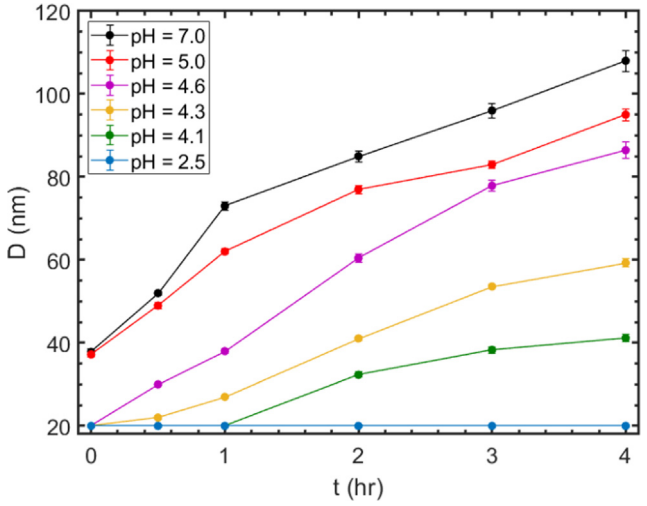

Fig. 8. The stability of the nanoemulsion at room temperature as a function of pH by monitoring the nanoemulsion droplet size over time. pH was adjusted using NaOH. See Fig. S4 for a long-time droplet size monitoring. The error bars are standard errors from 15 measurements.

Finally, we studied the effect of pH on the stability of the nanoemulsion by monitoring the size of droplets over a course of time. In this work, we used the phase inversion composition (PIC) method to synthesize the nanoemulsion. For the PIC method, or for any low-energy method to obtain nanoemulsions, the surfactant molecular geometry plays a crucial role in the formation of the droplet and the stability of the oil/water interface [6]. This molecular geometry is quantified by a quantity called packing parameter $p = a_T/a_H$, where a_T and a_H are the cross-sectional areas of the tail group and head group respectively. Different p values lead to different types of surfactant packing at the oil/water interface, and hence favor different curvature of the interface. The stability of the nanoemulsion at different pH is shown in Fig. 8. The pH was adjusted *after* the nanoemulsion synthesis. As shown, the increase in pH facilitates the instability of the nanoemulsion suspensions, whereas the pristine nanoemulsion stays stable throughout the experimental time window. As shown in Fig. 5B, increasing pH leads to the deprotonation of the carboxyl group of the surfactant on the droplets. Such deprotonation transforms the surfactant from being non-ionic (ζ ≈ 0 at low pH) to anionic (ζ < 0 at higher pH), and therefore changes p. This change in p ruptures the original packing of the surfactants at the oil/water interface, leading to an instability of the interface and therefore the

increase in the droplet size. Such instability highlights the importance of the molecular geometry of the surfactant in stabilizing the oil/water interface, and also suggests that in our system the increase in pH can be used as a strategy to demulsify the nanoemulsion droplets, that can be applied in practical applications such as in cosmetics [68,69], food industry [5,70], enhanced oil recovery [71–73] and water treatment [74].

From Fig. 8, we acknowledge that during the rheological characterization the size of the nanoemulsion droplets increases for pH values greater than 2.5. Thus, trends in the pH-responsive rheology in Fig. 7 are possibly convoluted with changes in droplet size. In order to decouple as much as possible pH changes in interactions from droplet size effects, we applied a fast temperature-ramp characterization (total measuring time ≈ 20 min in Fig. 6). Given this short amount of time, the change of size is limited (almost negligible for pH up to 4.3) and the thermally-gelling behavior can still take place since the droplet size is still in the nanoemulsion regime. In prior work we have extensively studied the effect of droplet size on a different thermally-gelling nanoemulsion system [25,26].

3.5. Effect of ionic strength on the rheological properties

The charged nature of the nanoemulsion droplets suggests the possibility to tune the gel properties using ionic strength. By screening the electrostatic repulsion using electrolytes, we expected the gelation of the nanoemulsion can be more easily induced at elevated temperatures. We again used the temperature-ramp rheology to study the effect of the ionic strength using sodium chloride (NaCl), and the result is shown in Fig. 9. As expected, the addition of NaCl facilitates the thermal gelation of the nanoemulsion where the increase in G′ and G″ takes place at lower temperatures. Moreover, the magnitude of the decrease in the viscoelastic moduli at the intermediate temperature is significantly reduced as more NaCl is added (e.g. the G′ value at 30 °C for [NaCl] = 1.0 M compared to that at ≈ 44 °C for [NaCl] = 0 M). Such reduction in the decline of moduli supports our proposed mechanism in which the charged carboxylate group on the droplet leads to an increase in electrostatic repulsion that disrupts the gel network. As more NaCl is added, the electrostatic repulsion is more greatly screened, leading to a lower gelation temperature and less reduction in the viscoelastic moduli at intermediate temperatures.

However, even for the highest ionic strength ([NaCl] = 1.0 M), the decrease in the viscoelastic moduli still exists. Moreover, the magnitude of the peak in the moduli is nearly the same across the [NaCl] window, suggesting repulsive interaction is still critical. As discussed earlier, the emergence of the electrostatic repulsion due to the thermally-triggered dissociation of the carboxyl group is responsible for the breakdown of the gel network (Figs. 1–3). Therefore, we hypothesized the addition of NaCl also facilitates the deprotonation of the carboxylic acids. Indeed, the effect of ionic strength on the dissociation of weak acids has been already studied in the literature. It has been found out that the addition of electrolytes promotes the deprotonation of various weak acids since the activity coefficients of the ionic species are highly sensitive to the ionic strength [75–78]. This promoted dissociation due to NaCl is validated in Fig. 10 where the temperature-dependent zeta potential of the nanoemulsion droplets, ζ, at elevated [NaCl] is measured. As [NaCl] increases, the dissociation of carboxyl acids takes place at lower temperatures and |ζ| at higher temperatures is also increased, which is consistent with prior studies where the electrolytes facilitate the weak acid dissociation [75–78]. Moreover, at higher [NaCl], ζ reaches a plateau at lower temperatures. This is consistent with the rheological data in Fig. 9 where the minimum in moduli takes place at lower temperatures for higher [NaCl], which also supports the proposed mechanism where the increase in electrostatic repulsion due to the weak acid dissociation is responsible for the decrease in the viscoelastic moduli.

We also note that, as shown in Fig. 9, at high ionic strength (NaCl = 1.0 M), the nanoemulsion can gel near room temperature. This early gelation is not intuitive since it seems to disagree with the discussion on the promoted carboxylic acid dissociation. Therefore, the addition of electrolyte must also modify the attractive interaction to induce an early onset of gelation. Indeed, prior studies have shown that the addition of the salts facilitates the association between PEG molecules [79–82]. The phase separation, or the cloud point, takes place at a lower temperature when more salts are added [79,81,82]. Therefore, in our system, the addition of NaCl enhances the attractive interaction resulting from the PEG-PEG association between the droplets, which also supports our proposed mechanism where the PEG_w-PEG_w association gives the inter-droplet attraction in our nanoemulsion suspension. We acknowledge that the effect of the ionic strength on the attraction and repulsion is interconnected. Future work will focus on the decoupling of the effect of the addition of electrolytes on the nanoemulsion gelation and the contribution to both attractive and repulsive interaction in a more quantitative fashion.

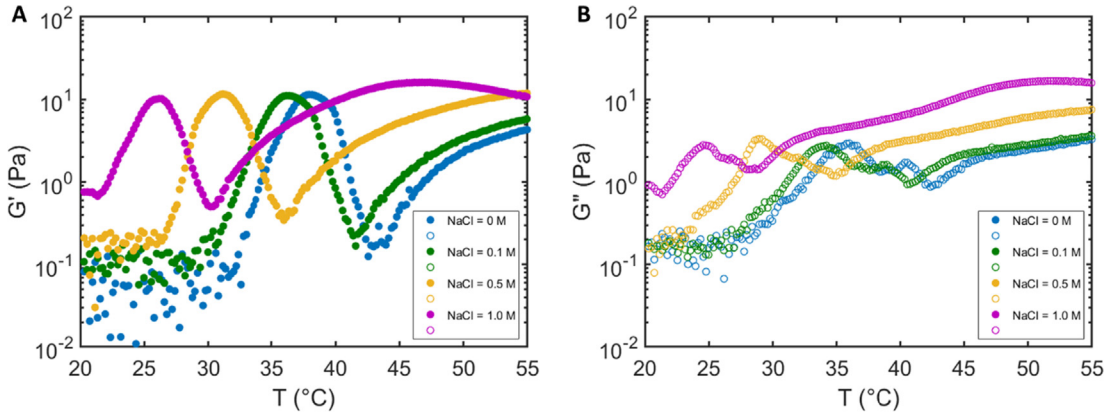

Fig. 9. Effect of the ionic strength on the rheological properties of the nanoemulsion (pH = 2.5) using SAOS at a fixed angular frequency = 25 rad/s. The figure shows (A) storage modulus, G′ and (B) loss modulus, G″ as a function of temperature, T, with increasing ionic strengths. The ionic strength was adjusted using NaCl as indicated in the figure.

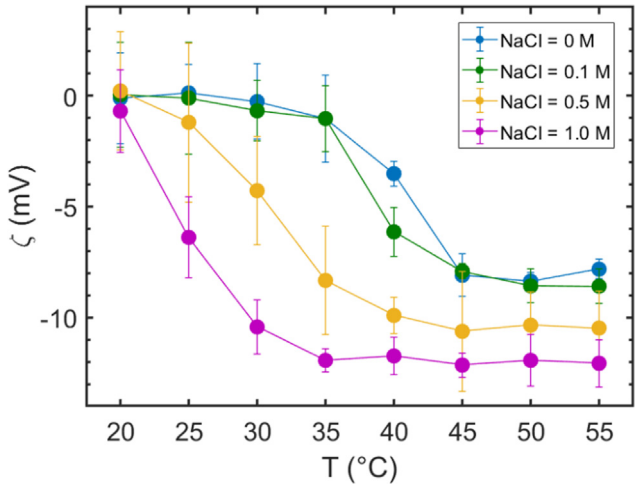

Fig. 10. Zeta potential (ζ) of the nanoemulsion droplets as a function of temperature (T) at elevated ionic strength. Ionic strength was adjusted using NaCl. The pH of the nanoemulsion is 3.1. The error bars are standard errors from 30 measurements.

4. Conclusion

Building of a molecular-scale understanding of our prior thermally-gelling nanoemulsion systems [25–27], in this work we develop a new nanoemulsion system in which the properties can be modulated through both temperature and pH. The nanoemulsion is synthesized using a low energy method, and the droplets are stabilized with weak acid surfactants containing poly(ethylene glycol) segments (PEG) and carboxyl groups. The association between the PEGs and the deprotonation of the carboxylic acids control the inter-droplet attractive and repulsive interactions. As the temperature is increased, the viscoelastic moduli of the nanoemulsion system first increase, then decrease and finally increase again. In a parallel fashion to the moduli trends, the gel network also experiences an initial formation, destruction and reformation as the temperature is increased. Such non-intuitive trends are due to attractive and repulsive interactions which both change as a function of temperature, as validated by zeta potential measurements and comparisons to prior research [43–46]. The dissociation of the carboxyl groups on the surfactant was further leveraged as a strategy to tune the nanoemulsion gel rheological properties by changing the pH of the system. Moreover, with an understanding of surfactant packing at the interface, we can further destabilize the nanoemulsion droplets by changing the surfactant packing parameter via pH [6]. Finally, we showed that the ionic strength of the system can be used as another engineering handle to tune the gel properties.

The presented work shows that subtle competition between attractive and repulsive interactions determines the system's properties, allowing researchers to design more complex nanoemulsion-based soft matter materials. Moreover, the mechanistic understanding of the interactive potentials at the molecular level provides various engineering strategies to manipulate the material properties. For example, the presented gelling nanoemulsions can be used in cosmetic products such as a skin cream – in the bottle the nanoemulsion system is a liquid at ambient temperature with good flowability, and the nanoemulsion can gel in contact with the skin due to a rise in temperature. Thereafter, a change of pH due to prolonged contact with the skin can disrupt the nanoemulsion gel network and the nano-sized droplets can then be easily absorbed into the skin [1,9]. Furthermore, the oil droplets are effective vehicles to encapsulate hydrophobic active ingredients [4,17]. In addition, a nanoemulsion system which responds to changes in both pH and temperature could find use in enhanced oil recovery applications where temperature and pH gradients can be found. Future work will focus on developing skincare products using the presented nanoemulsion system, and in developing a deeper quantitative understanding of the pairwise interactions between nanoemulsion droplets.

CRediT authorship contribution statement

Li-Chiun Cheng, Conceptualization, Data curation, Formal analysis, Investigation, Methodology, Resources, Software, Validation, Visualization, Writing - original draft, Writing - review editing. **Seyed Meysam Hashemnejad**, Conceptualization, Investigation, Methodology. **Brady Zarket**, Conceptualization. **Sivaramakrishnan Muthukrishnan**, Conceptualization, Funding acquisition. **Patrick S. Doyle**, Conceptualization, Data curation, Funding acquisition, Methodology, Project administration, Supervision, Writing - original draft, Writing - review editing.

Declaration of Competing Interest

P.S.D. acknowledges financial support from L'Oréal. B.Z. and S.M. are employees of L'Oréal. The remaining authors declare no competing interests.

Acknowledgement

We thank L'Oréal for partial financial support. L.-C. C is supported in part by the MRSEC Program of the National Science Foundation under award number DMR – 1419807 and the National Science Foundation grant CMMI – 1824297.

Appendix A. Supplementary material

Supplementary data to this article can be found online at https://doi.org/10.1016/j.jcis.2019.12.054.

References

[1] A. Gupta, H.B. Eral, T.A. Hatton, P.S. Doyle, Nanoemulsions: formation, properties and applications, Soft Matter 12 (2016) 2826–2841, https://doi.org/10.1039/C5SM02958A.
[2] N. Anton, J.-P. Benoit, P. Saulnier, Design and production of nanoparticles formulated from nano-emulsion templates—A review, J. Control. Release 128 (2008) 185–199, https://doi.org/10.1016/j.jconrel.2008.02.007.
[3] K. Landfester, Miniemulsion polymerization and the structure of polymer and hybrid nanoparticles, Angew. Chemie Int. Ed. 48 (2009) 4488–4507, https://doi.org/10.1002/anie.200900723.
[4] A.H. Saberi, Y. Fang, D.J. McClements, Thermal reversibility of vitamin E-enriched emulsion-based delivery systems produced using spontaneous emulsification, Food Chem. 185 (2015) 254–260, https://doi.org/10.1016/j.foodchem.2015.03.080.
[5] D.J. McClements, Food Emulsions, CRC Press, 2015.
[6] J.S. Komaiko, D.J. McClements, Formation of food-grade nanoemulsions using low-energy preparation methods: a review of available methods, Compr. Rev. Food Sci. Food Saf. 15 (2016) 331–352, https://doi.org/10.1111/1541-4337.12189.
[7] V. Mahendran, J. Philip, Sensing of biologically important cations such as Na +, K +, Ca 2+, Cu 2+, and Fe 3+ using magnetic nanoemulsions, Langmuir 29 (2013) 4252–4258, https://doi.org/10.1021/la400502b.
[8] V. Mahendran, J. Philip, Non-enzymatic glucose detection using magnetic nanoemulsions, Appl. Phys. Lett. 105 (2014), https://doi.org/10.1063/1.4896522.
[9] M.N. Yukuyama, D.D.M. Ghisleni, T.J.A. Pinto, N.A. Bou-Chacra, Nanoemulsion: process selection and application in cosmetics - a review, Int. J. Cosmet. Sci. 38 (2016) 13–24, https://doi.org/10.1111/ics.12260.
[10] L. Alison, S. Menasce, F. Bouville, E. Tervoort, I. Mattich, A. Ofner, A.R. Studart, 3D printing of sacrificial templates into hierarchical porous materials, Sci. Rep. 9 (2019) 409, https://doi.org/10.1038/s41598-018-36789-z.
[11] T.G. Mason, J.N. Wilking, K. Meleson, C.B. Chang, S.M. Graves, Nanoemulsions: formation, structure, and physical properties, J. Phys. Condens. Matter. 18 (2006) R635–R666, https://doi.org/10.1088/0953-8984/18/41/R01.

[12] M.E. Helgeson, Colloidal behavior of nanoemulsions: Interactions, structure, and rheology, Curr. Opin. Colloid Interface Sci. 25 (2016) 39–50, https://doi.org/10.1016/j.cocis.2016.06.006.
[13] J.N. Wilking, S.M. Graves, C.B. Chang, K. Meleson, M.Y. Lin, T.G. Mason, Dense cluster formation during aggregation and gelation of attractive slippery nanoemulsion droplets, Phys. Rev. Lett. 96 (2006) 015501, https://doi.org/10.1103/PhysRevLett. 96.015501.
[14] J. Kim, Y. Gao, C. Hebebrand, E. Peirtsegaele, M.E. Helgeson, Polymer–surfactant complexation as a generic route to responsive viscoelastic nanoemulsions, Soft Matter 9 (2013) 6897–6910, https://doi.org/10.1039/c3sm50301a.
[15] Y. Gao, J. Kim, M.E. Helgeson, Microdynamics and arrest of coarsening during spinodal decomposition in thermoreversible colloidal gels, Soft Matter 11 (2015) 6360–6370, https://doi.org/10.1039/C5SM00851D.
[16] L.C. Hsiao, A.Z.M. Badruddoza, L.-C. Cheng, P.S. Doyle, 3D printing of self-assembling thermoresponsive nanoemulsions into hierarchical mesostructured hydrogels, Soft Matter 13 (2017) 921–929, https://doi.org/10.1039/C6SM02208A.
[17] O. Sonneville-Aubrun, J.-T. Simonnet, F. L'Alloret, Nanoemulsions: a new vehicle for skincare products, Adv. Colloid Interface Sci. 108–109 (2004) 145–149, https://doi.org/10.1016/j.cis.2003.10.026.
[18] S. Asakura, F. Oosawa, Interaction between particles suspended in solutions of macromolecules, J. Polym. Sci. 33 (1958) 183–192, https://doi.org/10.1002/pol.1958.1203312618.
[19] H.N.W. Lekkerkerker, R. Tuinier, Colloids and the depletion interaction,, Springer, Netherlands, Dordrecht, 2011.
[20] V.V. Erramreddy, S. Ghosh, Influence of droplet size on repulsive and attractive nanoemulsion gelation, Colloids Surf. A Physicochem. Eng. Asp. 484 (2015) 144–152, https://doi.org/10.1016/j.colsurfa.2015.07.027.
[21] V.V. Erramreddy, S. Ghosh, Influence of emulsifier concentration on nanoemulsion gelation, Langmuir 30 (2014) 11062–11074, https://doi.org/10.1021/la502733v.
[22] P.C. Hiemenz, R. Rajagopalan, Principles of Colloid and Surface Chemistry, CRC Press, Taylor & Francis Group, 6000 Broken Sound Parkway NW, Suite 300, Boca Raton, FL 33487-2742, 1997.
[23] M.M. Fryd, T.G. Mason, Advanced Nanoemulsions, Annu. Rev. Phys. Chem. 63 (2012) 493–518, https://doi.org/10.1146/annurev-physchem-032210-103436.
[24] H.S. Kim, T.G. Mason, Advances and challenges in the rheology of concentrated emulsions and nanoemulsions, Adv. Colloid Interface Sci. 247 (2017) 397–412, https://doi.org/10.1016/j.cis.2017.07.002.
[25] M.E. Helgeson, S.E. Moran, H.Z. An, P.S. Doyle, Mesoporous organohydrogels from thermogelling photocrosslinkable nanoemulsions, Nat. Mater. 11 (2012) 344–352, https://doi.org/10.1038/nmta3248.
[26] L.-C. Cheng, Z.M. Sherman, J.W. Swan, P.S. Doyle, Colloidal gelation through thermally triggered surfactant displacement, Langmuir 35 (2019) 9464–9473, https://doi.org/10.1021/acs.langmuir.9b00596.
[27] S.M. Hashemnejad, A.Z.M. Badruddoza, B. Zarket, C. Ricardo Castaneda, P.S. Doyle, Thermoresponsive nanoemulsion-based gel synthesized through a low-energy process, Nat. Commun. 10 (2019) 2749, https://doi.org/10.1038/s41467-019-10749-1.
[28] M.E. Helgeson, Y. Gao, S.E. Moran, J. Lee, M. Godfrin, A. Tripathi, A. Bose, P.S. Doyle, Homogeneous percolation versus arrested phase separation in attractively-driven nanoemulsion colloidal gels, Soft Matter 10 (2014) 3122–3133, https://doi.org/10.1039/c3sm52951g.
[29] L.-C. Cheng, P.D. Godfrin, J.W. Swan, P.S. Doyle, Thermal processing of thermogelling nanoemulsions as a route to tune material properties, Soft Matter 14 (2018) 5604–5614, https://doi.org/10.1039/c8sm00814k.
[30] E. Lee, B. Kim, Smart delivery system for cosmetic ingredients using pH-sensitive polymer hydrogel particles, Korean J. Chem. Eng. 28 (2011) 1347–1350, https://doi.org/10.1007/s11814-010-0509-8.
[31] J. Hu, H. Meng, G. Li, S.I. Ibekwe, A review of stimuli-responsive polymers for smart textile applications, Smart Mater. Struct. 21 (2012), https://doi.org/10.1088/0964-1726/21/5/053001.
[32] N. Hashimah Alias, N. Aimi Ghazali, T. Amran Tengku Mohd, S. AdiebIdris, E. Yahya, N. Mohd Yusof, Nanoemulsion applications in enhanced oil recovery and wellbore cleaning: an overview, Appl. Mech. Mater. 754–755 (2015) 1161–1168, https://doi.org/10.4028/www.scientific.net/amm.754-755.1161.
[33] K.A. Whitaker, Z. Varga, L.C. Hsiao, M.J. Solomon, J.W. Swan, E.M. Furst, Colloidal gel elasticity arises from the packing of locally glassy clusters, Nat. Commun. 10 (2019) 2237, https://doi.org/10.1038/s41467-019-10039-w.
[34] L.C. Hsiao, P.S. Doyle, Celebrating Soft Matter's 10th Anniversary: Sequential phase transitions in thermoresponsive nanoemulsions, Soft Matter 11 (2015) 8426–8431, https://doi.org/10.1039/C5SM01581B.
[35] L.C. Hsiao, S. Pradeep, Experimental synthesis and characterization of rough particles for colloidal and granular rheology, Curr. Opin. Colloid Interface Sci. 43 (2019) 94–112, https://doi.org/10.1016/j.cocis.2019.04.003.
[36] J.C.-W. Lee, L. Porcar, S.A. Rogers, Unveiling temporal nonlinear structure-rheology relationships under dynamic shearing, Polym. (Basel) 11 (2019) 1189, https://doi.org/10.3390/polym11071189.
[37] J.C.-W. Lee, K.M. Weigandt, E.G. Kelley, S.A. Rogers, Structure-property relationships via recovery rheology in viscoelastic materials, Phys. Rev. Lett. 122 (2019) 248003, https://doi.org/10.1103/PhysRevLett. 122.248003.
[38] L. Kass, E.D. Cardenas-Vasquez, L.C. Hsiao, Composite double network hydrogels with thermoresponsive colloidal nanoemulsions, AIChE J. 65 (2019) 1–8, https://doi.org/10.1002/aic.16817.
[39] P. Fernandez, V. André, J. Rieger, A. Kühnle, Nano-emulsion formation by emulsion phase inversion, Colloids Surf. A Physicochem. Eng. Asp. 251 (2004) 53–58, https://doi.org/10.1016/j.colsurfa.2004.09.029.
[40] I. Solè, C.M. Pey, A. Maestro, C. González, M. Porras, C. Solans, J.M. Gutiérrez, Nano-emulsions prepared by the phase inversion composition method: Preparation variables and scale up, J. Colloid Interface Sci. 344 (2010) 417–423, https://doi.org/10.1016/j.jcis.2009.11.046.
[41] L.-C. Cheng, L.C. Hsiao, P.S. Doyle, Multiple particle tracking study of thermally-gelling nanoemulsions, Soft Matter 13 (2017) 6606–6619, https://doi.org/10.1039/c7sm01191a.
[42] J. Mewis, N.J. Wagner, Colloidal Suspension Rheology, Cambridge University Press, Cambridge, 2011.
[43] K. Sue, T. Usami, K. Arai, Determination of acetic acid dissociation constants to 400 °C and 32 MPa by potentiometric pH measurements, J. Chem. Eng. Data. 48 (2003) 1081–1084, https://doi.org/10.1021/je030142j.
[44] K. Sue, F. Ouchi, K. Minami, K. Arai, Determination of carboxylic acid dissociation constants to 350 °C at 23 MPa by potentiometric pH measurements, J. Chem. Eng. Data. 49 (2004) 1359–1363, https://doi.org/10.1021/je049923q.
[45] H.S. Harned, R.W. Ehlers, The dissociation constant of propionic acid from 0 to 60°, J. Am. Chem. Soc. 55 (1933) 2379–2383, https://doi.org/10.1021/ja01333a024.
[46] G.A. Poskrebyshev, P. Neta, R.E. Huie, Temperature dependence of the acid dissociation constant of the hydroxyl radical, J. Phys. Chem. A. 106 (2002) 11488–11491, https://doi.org/10.1021/jp020239x.
[47] V. Ferrari, D.J. Cutler, Temperature dependence of the acid dissociation constants of chloroquine, J. Pharm. Sci. 76 (1987) 554–556, https://doi.org/10.1002/jps.2600760714.
[48] K.C. Tam, E. Wyn-Jones, Insights on polymer surfactant complex structures during the binding of surfactants to polymers as measured by equilibrium and structural techniques, Chem. Soc. Rev. 35 (2006) 693, https://doi.org/10.1039/b415140m.
[49] R.D. Lundberg, F.E. Bailey, R.W. Callard, Interactions of inorganic salts with poly(ethylene oxide), J. Polym. Sci. Part A-1 Polym. Chem. 4 (1966) 1563–1577, https://doi.org/10.1002/pol.1966.150040620.
[50] B. Cabane, R. Duplessix, Neutron scattering study of water-soluble polymers adsorbed on surfactant micelles, Colloids Surf. 13 (1985) 19–33, https://doi.org/10.1016/0166-6622(85)80003-2.
[51] S. Dai, K.C. Tam, Isothermal titration calorimetry studies of binding interactions between polyethylene glycol and ionic surfactants, J. Phys. Chem. B. 105 (2001) 10759–10763, https://doi.org/10.1021/jp0110354.
[52] L. Bernazzani, S. Borsacchi, D. Catalano, P. Gianni, V. Mollica, M. Vitelli, F. Asaro, L. Feruglio, On the interaction of sodium dodecyl sulfate with oligomers of poly (Ethylene Glycol) in aqueous solution, J. Phys. Chem. B. 108 (2004) 8960–8969, https://doi.org/10.1021/jp049673k.
[53] R. Mészáros, I. Varga, T. Gilányi, Effect of polymer molecular weight on the polymer/surfactant interaction, J. Phys. Chem. B. 109 (2005) 13538–13544, https://doi.org/10.1021/jp051272x.
[54] Y.J. Nikas, D. Blankschtein, Complexation of nonionic polymers and surfactants in dilute aqueous solutions, Langmuir 10 (1994) 3512–3528, https://doi.org/10.1021/la00022a026.
[55] R.D. Groot, Mesoscopic simulation of polymer−surfactant aggregation, Langmuir 16 (2000) 7493–7502, https://doi.org/10.1021/la000010d.
[56] H. Bao, L. Li, L.H. Gan, H. Zhang, Interactions between ionic surfactants and polysaccharides in aqueous solutions, Macromolecules 41 (2008) 9406–9412, https://doi.org/10.1021/ma801957v.
[57] Y. Li, R. Xu, D.M. Bloor, J. Penfold, J.F. Holzwarth, E. Wyn-Jones, Moderation of the interactions between sodium dodecyl sulfate and poly(vinylpyrrolidone) using the nonionic surfactant hexaethyleneglycol Mono- n -dodecyl Ether C 12 EO 6: an electromotive force microcalorimetry, and small-angle neutron scattering study, Langmuir 16 (2000) 8677–8684, https://doi.org/10.1021/la000292h.
[58] M. Almgren, J. Van Stam, C. Lindblad, P. Li, P. Stilbs, P. Bahadur, Aggregation of poly(ethylene oxide)-poly(propylene oxide)-poly(ethylene oxide) triblock copolymers in the presence of sodium dodecyl sulfate in aqueous solution, J. Phys. Chem. 95 (1991) 5677–5684, https://doi.org/10.1021/j100167a055.
[59] M. Bjoerling, G. Karlstroem, P. Linse, Conformational adaption of poly(ethylene oxide): a carbon-13 NMR study, J. Phys. Chem. 95 (1991) 6706–6709, https://doi.org/10.1021/j100170a060.
[60] W.F. Polik, W. Burchard, Static light scattering from aqueous poly(ethylene oxide) solutions in the temperature range 20–90°C, Macromolecules 16 (1983) 978–982, https://doi.org/10.1021/ma00240a030.
[61] R. Kjellander, E. Florin, Water structure and changes in thermal stability of the system poly(ethylene oxide)–water, J. Chem. Soc. Faraday Trans. 1 Phys. Chem. Condens. Phases. 77 (1981) 2053, https://doi.org/10.1039/f19817702053.
[62] G. Karlstroem, A new model for upper and lower critical solution temperatures in poly(ethylene oxide) solutions, J. Phys. Chem. 89 (1985) 4962–4964, https://doi.org/10.1021/j100269a015.
[63] G. Karlstroem, A. Carlsson, B. Lindman, Phase diagrams of nonionic polymer-water systems: experimental and theoretical studies of the effects of surfactants and other cosolutes, J. Phys. Chem. 94 (1990) 5005–5015, https://doi.org/10.1021/j100375a045.
[64] S. Hocine, M.H. Li, Thermoresponsive self-assembled polymer colloids in water, Soft Matter 9 (2013) 5839–5861, https://doi.org/10.1039/c3sm50428j.

[65] H. Hoekstra, J. Mewis, T. Narayanan, J. Vermant, Multi length scale analysis of the microstructure in sticky sphere dispersions during shear flow, Langmuir 21 (2005) 11017–11025, https://doi.org/10.1021/la051488q.
[66] A.P.R. Eberle, R. Castañeda-Priego, J.M. Kim, N.J. Wagner, Dynamical arrest, percolation, gelation, and glass formation in model nanoparticle dispersions with thermoreversible adhesive interactions, Langmuir 28 (2012) 1866–1878, https://doi.org/10.1021/la2035054.
[67] D. Hui, M. Nawaz, D.P. Morris, M.R. Edwards, B.R. Saunders, Study of pH-triggered heteroaggregation and gel formation within mixed dispersions, J. Colloid Interface Sci. 324 (2008) 110–117, https://doi.org/10.1016/j.jcis.2008.05.035.
[68] Y. Arai, H. Nakajima, K. Ohno, F. Application, P. Data, P. Examiner, A. Diamond, Emulsion for Hair Treatment, USOO5817155A, 1998.
[69] J. Tang, P.J. Quinlan, K.C. Tam, Stimuli-responsive Pickering emulsions: recent advances and potential applications, Soft Matter 11 (2015) 3512–3529, https://doi.org/10.1039/C5SM00247H.
[70] T.P. Sari, B. Mann, R. Kumar, R.R.B. Singh, R. Sharma, M. Bhardwaj, S. Athira, Preparation and characterization of nanoemulsion encapsulating curcumin, Food Hydrocoll. 43 (2015) 540–546, https://doi.org/10.1016/j.foodhyd.2014.07.011.
[71] M. Rondón, P. Bouriat, J. Lachaise, J.-L. Salager, Breaking of water-in-crude oil emulsions. 1. Physicochemical phenomenology of demulsifier action, Energy Fuels 20 (2006) 1600–1604, https://doi.org/10.1021/ef060017o.
[72] C.W. Angle, Y. Hua, Phase separation and interfacial viscoelasticity of charge-neutralized heavy oil nanoemulsions in water, J. Chem. Eng. Data. 56 (2011) 1388–1396, https://doi.org/10.1021/je101162n.
[73] A.K. Fraga, L.F.I. Souza, J.R. Magalhães, C.R.E. Mansur, Development and evaluation of oil in water nanoemulsions based on polyether silicone as demulsifier and antifoam agents for petroleum, J. Appl. Polym. Sci. 131 (2014), https://doi.org/10.1002/app.40889.
[74] F. Shehzad, I.A. Hussein, M.S. Kamal, W. Ahmad, A.S. Sultan, M.S. Nasser, Polymeric surfactants and emerging alternatives used in the demulsification of produced water: a review, Polym. Rev. 58 (2018) 63–101, https://doi.org/10.1080/15583724.2017.1340308.
[75] M.D. Seymour, Q. Fernando, Effect of ionic strength on equilibrium constants, J. Chem. Educ. 54 (1977) 225, https://doi.org/10.1021/ed054p225.
[76] C. Rey-Castro, R. Herrero, M.E. Sastre de Vicente, Gibbs-Donnan and specific-ion interaction theory descriptions of the effect of ionic strength on proton dissociation of alginic acid, J. Electroanal. Chem. 564 (2004) 223–230, https://doi.org/10.1016/j.jelechem.2003.10.023.
[77] M.E. Krahl, The effect of variation in ionic strength and temperature on the apparent dissociation constants of thirty substituted barbituric acids, J. Phys. Chem. 44 (1940) 449–463, https://doi.org/10.1021/j150400a010.
[78] D.A. Dikin, M. Mehta, C.W. Bark, C.M. Folkman, C.B. Eom, V. Chandrasekhar, Coexistence of superconductivity and ferromagnetism in two dimensions, Phys. Rev. Lett. 107 (2011) 056802, https://doi.org/10.1103/PhysRevLett.107.056802.
[79] M. Ataman, E.A. Boucher, Properties of aqueous salt solutions of poly(ethylene oxide), J. Polym. Sci. Polym. Phys. Ed. 20 (1982) 1585–1592, https://doi.org/10.1002/pol.1982.180200907.
[80] B. Briscoe, P. Luckham, S. Zhu, On the effects of water solvency towards non–ionic polymers, Proc. R. Soc. London. Ser. A Math. Phys. Eng. Sci. 455 (1999) 737–756, https://doi.org/10.1098/rspa.1999.0332.
[81] E.A. Boucher, P.M. Hines, Effects of inorganic salts on the properties of aqueous poly(ethylene oxide) solutions, J. Polym. Sci. Polym. Phys. Ed. 14 (1976) 2241–2251, https://doi.org/10.1002/pol.1976.180141209.
[82] K.P. Ananthapadmanabhan, E.D. Goddard, Aqueous biphase formation in polyethylene oxide-inorganic salt systems, Langmuir 3 (1987) 25–31, https://doi.org/10.1021/la00073a005.